In-Plane Shear Behavior of SC Composite Walls: Theory vs. Experiment

Amit H. Varma[1], Kai Zhang[2], Hoseok Chi[3], Peter Booth[4], Tod Baker[5]
[1]Associate Professor, School of Civil Engineering, Purdue University, West Lafayette, IN, ahvarma@purdue.edu
[2]PhD Candidate, School of Civil Engineering, Purdue University, West Lafayette, IN, kai-zh@purdue.edu
[3]Research Scientist, Bowen Lab, Purdue University, West Lafayette, hchi@purdue.edu
[4]PhD Candidate, School of Civil Engineering, Purdue University, West Lafayette, IN, boothpn@purdue.edu
[5]Fellow Engineer, Westinghouse Electric Corporation, Cranberry Township, PA, bakerth@westinghouse.com

ABSTRACT

The in-plane shear behavior of steel-plate composite (SC) walls is different from that of reinforced concrete (RC) walls with orthogonal grids of longitudinal and transverse rebar. In SC walls, the steel plates contribute not only their longitudinal and transverse strength, but also there in-plane shear stiffness and strength to the behavior of the composite section. The in-plane shear loading produces principal tension and compression forces in the composite SC section. The principal tension causes the concrete to crack, and after cracking the concrete sandwich behaves like an orthotropic plate with negligible stiffness in the principal tension direction but significant stiffness and compressive strength in the principal compression direction.

This paper presents a simple mechanistic representation of this complex in-plane shear behavior of SC composite walls, and a design equation for calculating their in-plane shear stiffness and strength. These equations are compared and evaluated using existing experimental results. Additionally, these equations are further confirmed by conducting a large-scale in-plane shear test using a unique test setup and approach. The experimental results included the measured cyclic shear force-strain response of the SC panel, the shear strains, and the principal strains measured in the steel plates. The experimental results are shown to verify the behavior theory.

INTRODUCTION

There is considerable interest in the use of steel plate composite (SC) walls for safety related nuclear facilities that are part of third generation nuclear power plants. SC construction can potentially be more efficient than reinforced concrete from construction scheduling and structural efficiency standpoints. The in-plane shear behavior of these SC walls is the primary lateral load resisting mechanism in these structures.

The in-plane shear behavior of the SC composite wall is governed by the plane stress behavior of the steel faceplates, and the orthotropic elastic behavior of concrete cracked in principal tension. The steel headed studs provide composite action by anchoring the steel faceplates to the concrete sandwich. The deformed wire tie bars also provide composite action, but most importantly they provide structural integrity to keep the composite section together. The steel-headed studs and the tie bars provide a secondary but important function to the in-plane shear behavior of SC composite wall.

BACKGROUND

Conducting pure in-plane shear tests is extremely challenging, and there are only a few laboratories in the world capable of subjecting wall panels to pure in-plane shear loading to determine their fundamental behavior and cyclic performance. Ozaki et al. [1] have conducted such pure in-plane shear tests on SC wall panels using specially designed test setup and specimens. The test setup was capable of subjecting SC wall panel specimens to cyclic in plane shear loading. The test specimens were 47.25 x 47.25 in. in plan, and 7.875 in. in thickness. The specimens had special grip regions at the edges to facilitate the application of in-plane shear forces.

Table 1 summarizes the details of three of the specimens tested by Ozaki et al. [1] by subjecting them to pure in-plane shear. It is important to note that Ozaki et al. [1] tested several more specimens subjected to slight axial compression combined with in-plane shear that are not discussed further here. As shown in Table 1, the plate slenderness (s/t_s) defined by the spacing of the shear connectors and the thickness of the steel plates was approximately equal to 30. The primary variable between the three specimens was the steel plate thickness (t_s), which also represents the steel reinforcement ratio (calculated at $2t_s/T$). The steel plate reinforcement ratios were approximately equal to 2.3%, 3.2%, and 4.5% for Specimens S2-00-NN, S3-00-NN, and S4-00-NN, respectively.

Table 1. Details of Pure In-Plane Shear Specimens Tested by Ozaki et al. [1]

Specimen	Plate thickness (t_s) in.	Stud diameter (d) in.	Stud spacing (s)	s/t_s	F_y (ksi)	f'_c (ksi)
S2-00-NN	0.09	0.16	2.76	30	49.3	6.1
S3-00-NN	0.13	0.20	3.94	31	50.9	6.1
S4-00-NN	0.18	0.35	5.31	30	50.2	6.2

The specimens were subjected to cyclic shear strain γ_{xy} history consisting of cycles at 0.5, 1.0, 2.0, 3.0, 4.0, 6.0, and 20 x 10^{-3}. The envelope of the cyclic hysteresis rules for Specimens S2-00-NN, S3-00-NN, and S4-00-NN are show in Figure 1. Table 2 shows numerical values of the experimental results for specimens S2-00-NN, S3-00-NN, and S4-00-NN subjected to pure in-plane shear loading. It includes the measured the pre-cracking stiffness (K_{xy}^{uncr}), cracking shear force (S_{ct}), post-cracking shear stiffness (K_{xy}^{cr}), and the shear strength corresponding to the limit state of steel plate yielding (S_{xy}^{Y}) for the specimens.

Table 2. Experimental Results from Ozaki et al. [1] and and Comparisons with Analytical Values

	Experimental Results				Experimental Results / Analytical Values			
Specimen	K_{xy}^{uncr} (kips)	S_{ct} (kips)	K_{xy}^{cr} (kips)	S_{xy}^{Y} (kips)	K_{xy}^{uncr} / K_{xy}^{uncr}	S_{ct} / S_{ct}	K_{xy}^{cr} / K_{xy}^{cr}	S_{xy}^{Y} / S_{xy}^{Y}
S2-00-NN	668082	65.8	224131	514.1	0.85	1.02	1.10	1.18
S3-00-NN	695020	69.8	262922	689.2	0.85	1.04	1.00	1.14
S4-00-NN	883592	78.3	442873	788.0	1.02	1.10	1.30	0.98

The experimental results indicated that as the steel plate becomes thicker, the post-cracking shear modulus, the yield strength, and the maximum strength become higher, and the shear strain at maximum strength becomes smaller. Overall, all the specimens showed good behavior and ductility. The ultimate shear strain reached and exceeded at least 6.0 x 10^{-3} under cyclic loading.

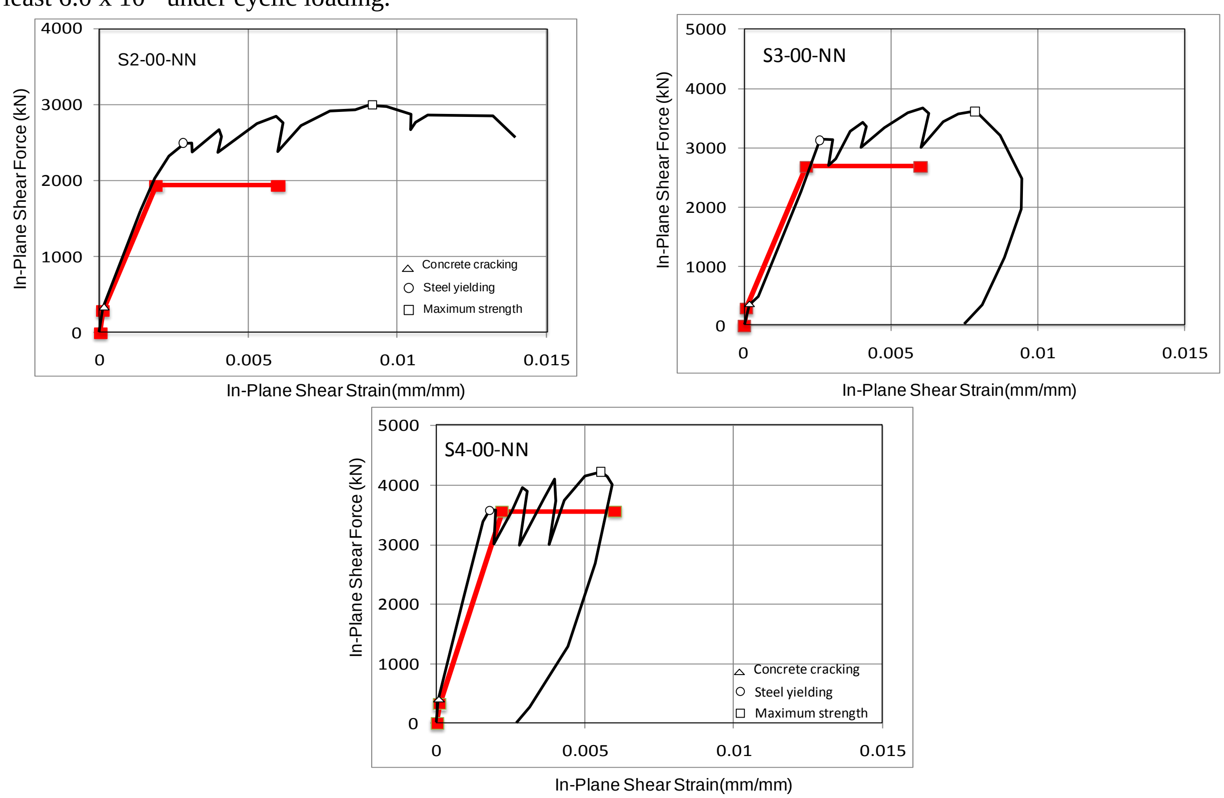

Figure 1. Experimental results from Ozaki [1] tests, and comparison with analytical model

MECHANICS BASED THEORY

The in-plane shear behavior of SC composite walls can be predicted using composite plate theory, while assuming (i) isotropic elastic plane-stress behavior for the steel faceplates, (ii) isotropic elastic behavior for the concrete sandwich before cracking, (iii) orthotropic elastic behavior of the concrete sandwich after cracking with zero stiffness in the principal tensile direction perpendicular to cracking, and 70 percent of the elastic stiffness for the principal compressive direction parallel to cracking, and (iv) Von Mises yield criterion for the steel faceplates.

The fundamental in-plane behavior of SC composite walls has been developed by Ozaki et al. [1], and also by Varma and Malushte [2]. The in-plane shear strength of SC composite walls can be estimated as the tri-linear shear force –strain curve shown in Figure 2.

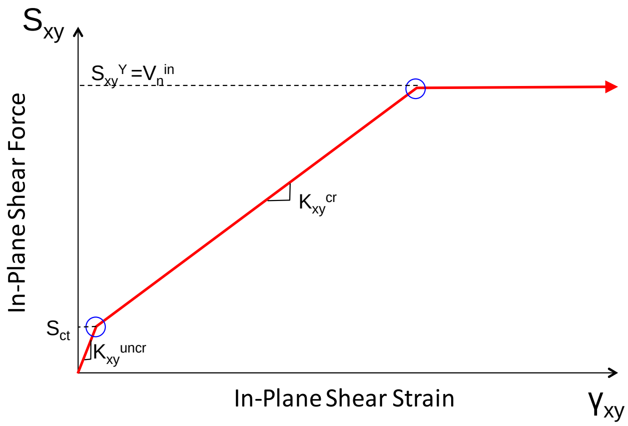

$$K_{xy}^{uncr} = G_s A_s + G_c A_c \qquad \textit{Equation 1}$$

$$S_{ct} = \frac{2\sqrt{f'_c}}{1000}\left(\frac{E_c A_c + E_s A_s}{E_c}\right) \qquad \textit{Equation 2}$$

$$K_{xy}^{cr} = K_{sc} + K_s = \frac{1}{\dfrac{4}{0.7E_c A_c} + \dfrac{2(1-\nu_s)}{E_s A_s}} + G_s A_s \qquad \textit{Equation 3}$$

$$S_{xy}^{Y} = V_n^{in} = \frac{K_s + K_{sc}}{\sqrt{3K_s^2 + K_{sc}^{\ 2}}} \times A_s F_y \qquad \textit{Equation 4}$$

Figure 2. In-Plane shear Behavior Model

The first part of the curve is before concrete cracking occurs. The in-plane shear stiffness (K_{xy}^{uncr}) can be estimated using that of the composite section shown in Equation 1. Concrete cracking occurs when the applied shear force (S_{xy}) exceeds the cracking threshold (S_{ct}), which can be calculated using Equation 2. The cracking threshold (S_{ct}) corresponds to a concrete principal tensile stress (in psi) of $2(f'_c)^{0.5}$, where f'_c is the compressive strength in psi.

The second part of the curve is after concrete cracking but before steel plate yielding. The in-plane shear stiffness (K_{xy}^{cr}) can be estimated as that of composite section with orthotropic properties for the 45^o cracked concrete (K_{sc}) and plane stress properties of the steel plate (K_s), see Equation 3.

The third part of the curve corresponds to the onset of steel plate Von Mises yielding, which occurs when the applied in-plane shear reaches S_{xy}^{Y} or V_n^{in} given by Equation 4. In Equations 1 to 4, G_s, E_s, and A_s are the shear modulus, elastic modulus, poisson ratio, and area of the steel in the composite section. G_c, E_c, and A_c are the shear modulus, elastic modulus, and area of the concrete in the section.

This mechanics based behavior model is summarized briefly in Figure 3, which shows critical steps in the derivation of the model and Equations 1-4 above. The model is presented in more detail in Varma and Malushte [2], and not repeated here for brevity. Figure 3 shows (a) the in-plane forces and strains, (b) the corresponding principal forces and strains, (c) resulting concrete cracking and orthotropic behavior, (d) composite section force equilibrium equation after cracking, (e) the free body diagram for section force equilibrium, and (f) the resulting steel and concrete stresses in the x and y directions. These resulting steel stresses were used to establish the occurrence of Von Mises yielding of the steel plates, which resulted in Equation 4 for the in-plane shear strength.

Figure 1 includes comparisons of the in-plane shear model shown in Figure 2 with the experimental results from Ozaki et al. [1]. Numerical comparisons of the pre-cracking shear stiffness (K_{xy}^{uncr}), cracking threshold (S_{ct}), post-cracking shear stiffness (K_{xy}^{cr}), and in-plane shear strength (S_{xy}^{Y}) are included in Table 2. The comparisons in Figure 2 and Table 2 indicate that the in-plane shear model is a reasonable and conservative representation of the in-plane shear behavior of SC walls with s/t_s ratios less than or equal to 30 and reinforcement ratios up to 4.5%.

In order to further verify the in-plane shear model, a unique large-scale in-plane shear test was conducted at Purdue University, Bowen Laboratory as explained in the following sub-sections.

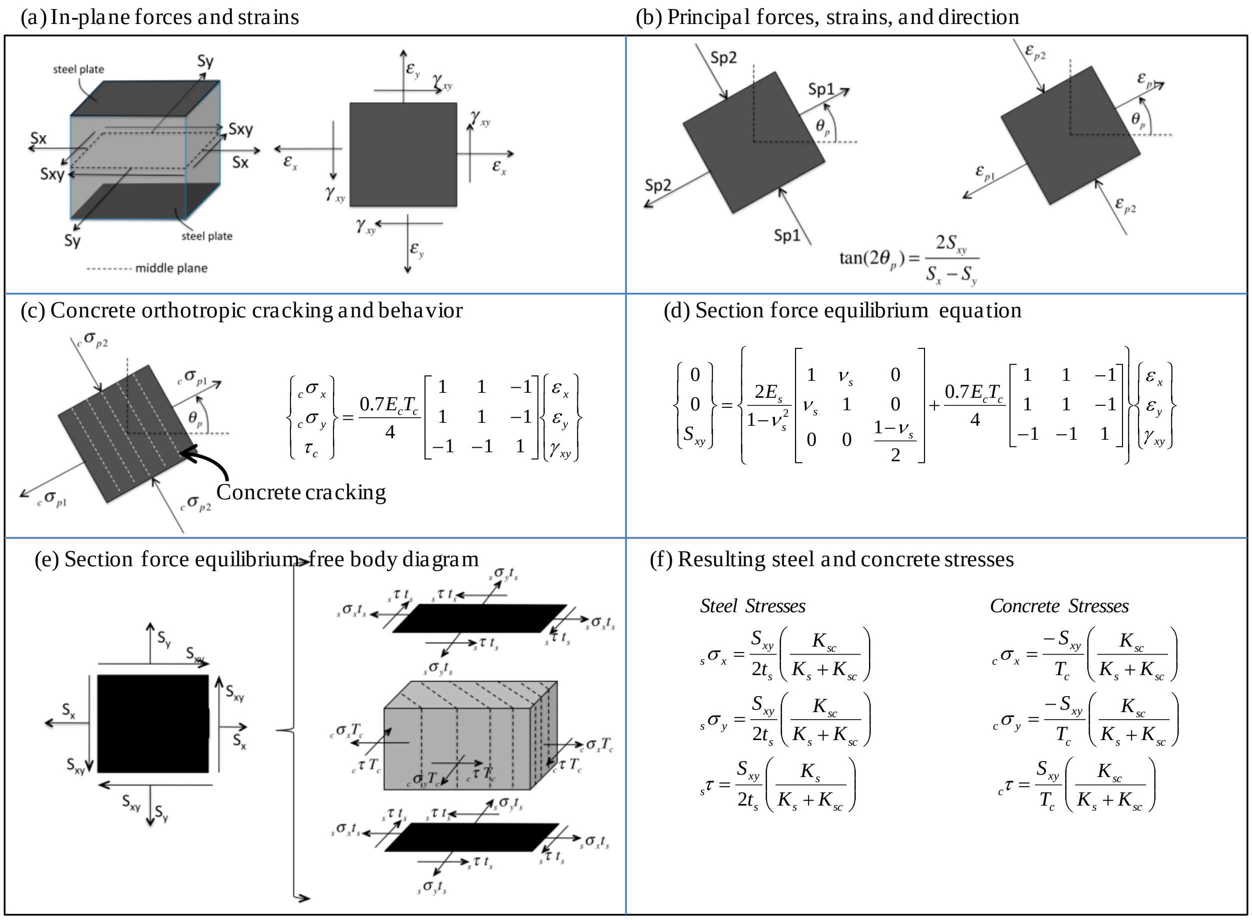

Figure 3 Summary of in-plane shear behavior theory

SPECIMEN DETAILS

A large-scale in-plane shear test was conducted to demonstrate the cyclic behavior and ductility of SC composite walls and to verify the mechanics based model. The thickness of the SC composite wall specimens is denoted as *T*. The thickness of steel faceplates was equal to t_s, and the nominal yield stress was equal to 50 ksi. The steel plate reinforcement ratio ($2t_s/T$) was equal to 4.16%. Shear connectors were welded to the steel plates with a spacing of 11.33 times of plate thickness (s/t_s =11.33). The nominal compression strength of infill concrete was equal to 6000 psi, and it was made from 0.75-inch aggregate.

The specimen was a flanged shear wall with one web and two identical flanges. The web represented the SC composite wall panel subjected to in-plane shear, and the flange walls were designed to resist the corresponding overturning moment. Figure 4 shows a picture of the test setup with specimen in place. The two concrete blocks at the bottom were first post-tensioned to the specimen web. Then, the concrete blocks were post-tensioned down to the reaction floor through holes in a steel base plate. The specimen flanges were further pre-tensioned to the steel base plate through holes in the concrete bottom blocks to prevent decompression due to the overturning moment. Thus, the flanges were designed to resist the applied overturning moment, and have minimal (if any) contribution to the in-plane shear, which was resisted by the SC wall specimen web.

All the post-tensioning was verified to ensure minimum losses. The specimen was cast along with a concrete top block, where the concrete block and connection were designed to transfer the applied shear force and moment, if there is any, to the specimen. The in-plane shear force was applied using four double-acting hydraulic rams. Each ram had 1000 kip capacity for push and 630-kip capacity for pull forces and 12-inch displacement stroke. The rams were attached with clevis and pin details at both ends to prevent restraints, and to large steel beams to spread the forces to the reaction wall. Electronic pressure transducers were used to measure the loads applied by the hydraulic rams.

Figure 4 Photograph of In-Plane Specimen and Setup

The test was terminated when the applied force approached 1200 kips, which was the design capacity for safe operation of the test setup. Excessive slippage of the setup on the laboratory floor was observed at the peak load.

INSTRUMENTATON

Displacement transducers were used to measure the horizontal and vertical displacements of the specimen, setup, the elongation and shortening of the web diagonals, and thus the shear strain of the specimen. Clinometers were attached to measure the rotations of the top and bottom concrete blocks and of the specimen. Strain gage rosettes and strain gages were glued to measure longitudinal, transverse, and shear strains at various locations in the steel plates, and strains in the tie bars. Instrumentation of the specimen is shown in Figure 5 (a) - (c).

As shown, the horizontal displacement as the base of the specimen just above the concrete blocks was measured using DT17. The horizontal displacement just above the test region of the specimen was measured using DT18. The horizontal displacement at the mid-height of the block was measured using DT19. Thus, DT18-DT17 measures the horizontal displacement (drift) of the 43 in. high test region of the specimen. Similarly DT19-DT17 also measures the drift of the specimen.

The rotations of the bottom concrete blocks are measured using DC1 and DC2. The rotation of the top concrete block was measured using DC3. Figure 5 (b) shows the strain gage layout for the west face of the specimen web. As shown, five points on the west face were instrumented with rectangular strain rosettes featuring three strain gages each. The grid of strain gage rosettes covered an approximately 30 x 30 in. region of the specimen web.

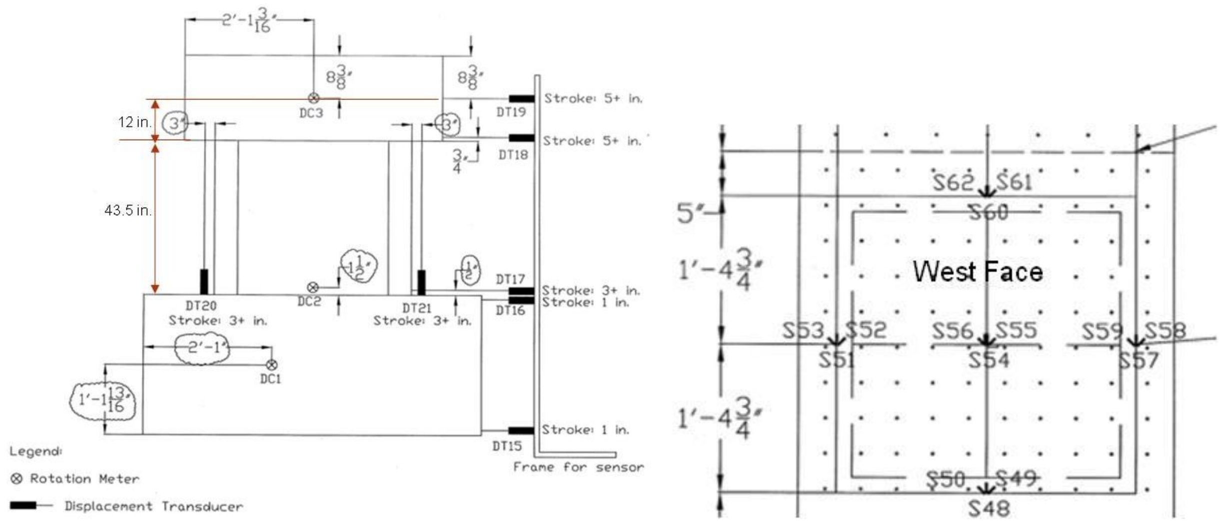

(a) Sensor Layout for Displacements and Rotations (b) Strain Gage Layout for West Face of Web

Figure 5 Instrumentation of SC Composite Wall Specimen

TEST RESULTS

The horizontal drifts (DT18-DT17) were corrected to account for the measured base rotation, and the interstory drift ratios were calculated. Figure 6 shows the measured lateral load – interstory drift ratio for the specimen.

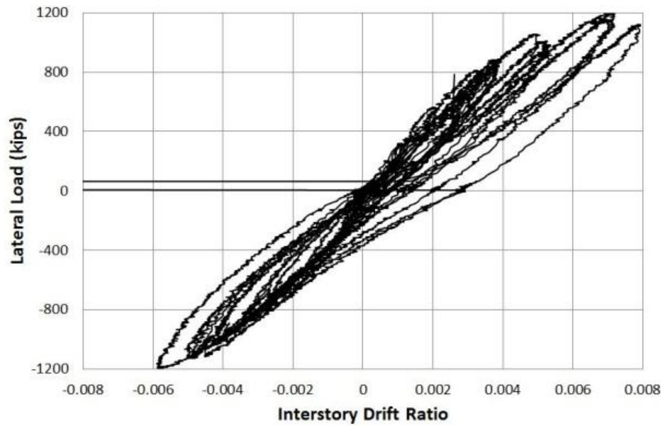

Figure 6. Shear Force – Interstory Drift Ratio Curve

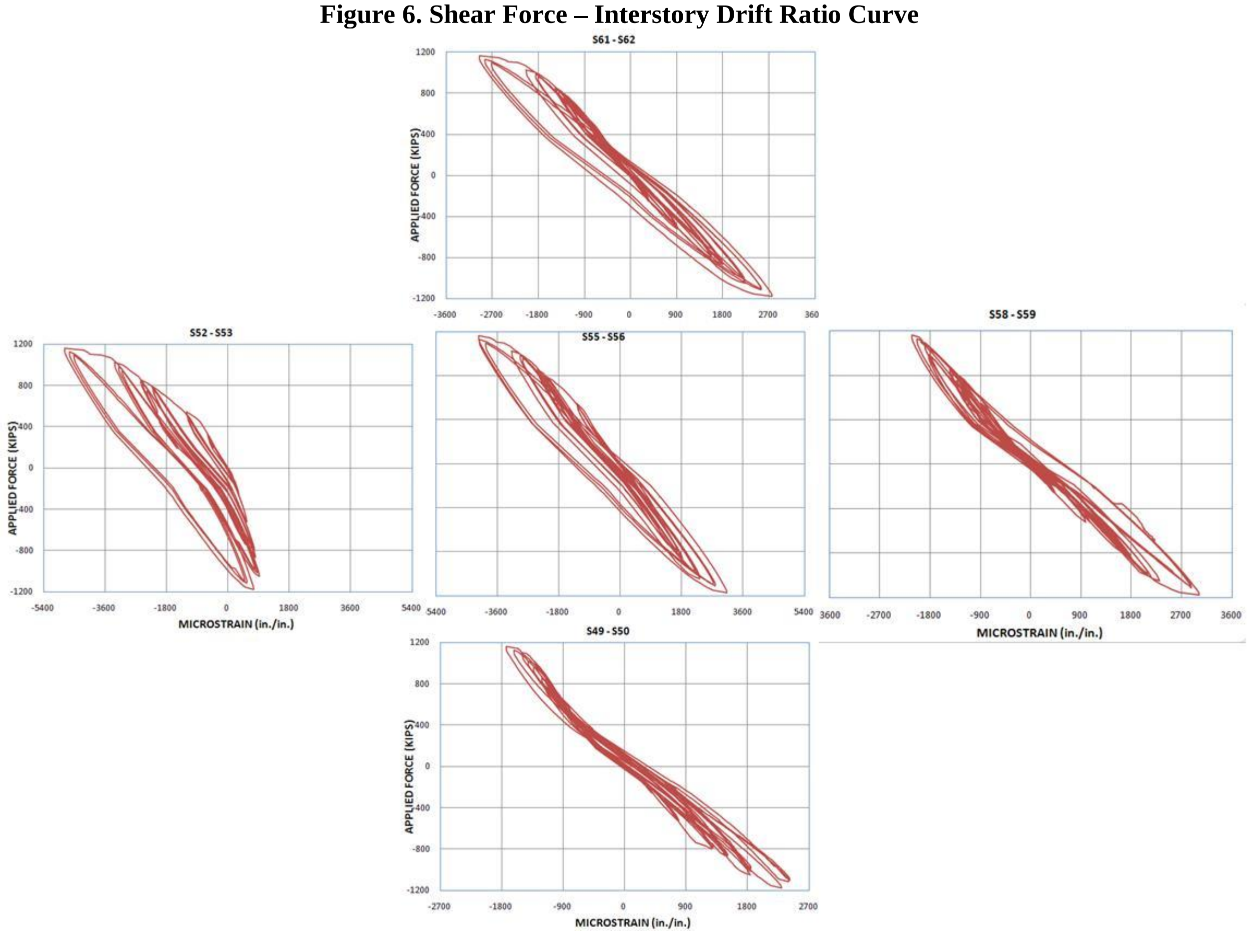

Figure 7 Measured Shear Strain on Specimen Webs

Figure 7 shows the shear strains measured on the west face of the web. The strains are shown in micro-strains, which is the actual strain value multiplied by 10^6. These shear strains were estimated as the difference between the measured diagonal strains at each point. The strains measured by the rectangular rosettes were corrected to account for the effects of transverse strain sensitivity using equations in the literature. The corrected strain values were used to further compute the principal directions with reference to the vertical axis, the principal strains, and the maximum shear strain as the difference between the principal strains.

The calculations indicate that as expected the principal directions varied approximately between -45 degree for push (+) force and +45 degree for the pull (-) forces. The calculated principal strains were quite comparable to the measured diagonal strains, and the maximum shear strain was also approximately equal to the difference between the measured diagonal strains. Figure 8 shows the principal directions, principal strains and maximum shear strains calculated for the points located at web center on both the east and west faces.

Additionally, the strain values on opposite steel plates of the same flange were demonstrated to be quite comparable to each other. This implies that the flanges are subjected to axial tension and compression with very little flexural bending (and shear). Thus, the specimen flanges carry axial tension and compression to help resist the overturning moment in the specimen, and their contribution to resisting the in-plane shear force applied to the specimen is minimal.

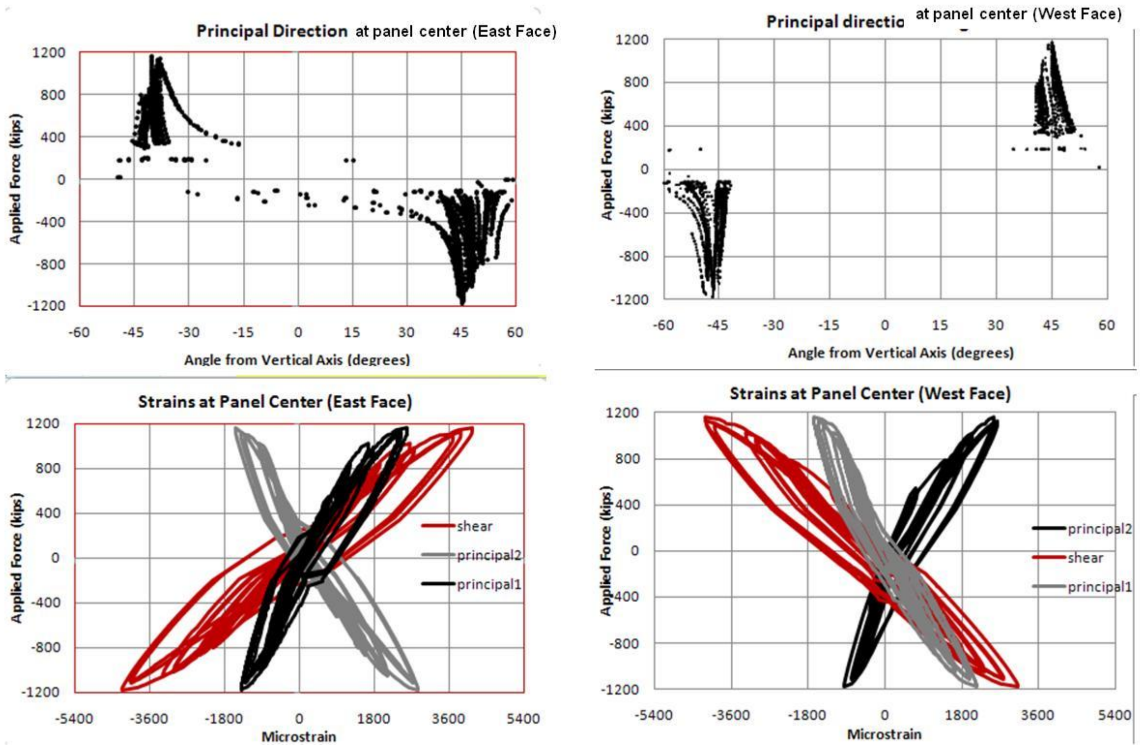

Figure 8 Principal Direction and Strains at Web Center (East and West Faces)

VERIFICATION

The in-plane shear behavior of the SC wall specimen can be estimated using the mechanics based theory shown in Figure 2. Figure 9 shows comparisons of the experimentally measured in-plane shear force-strain behavior with the behavior shown in Figure 2. The measured values of the steel yield stress (60.7 ksi) and concrete compressive strength (8200 psi) were used to estimate the in-plane shear behavior prediction.

The comparisons use the average in-plane shear behavior estimated using the displacement transducers in the web region. The comparisons shown in Figure 9 are quite favorable, but with some discrepancies. The experimental behavior does not seem to have a clear uncracked portion response, which is probably due to the cyclic nature of loading and locked in shrinkage strains. The experimental behavior seems to indicate point-wise inelasticity for some of the locations in the web, which is probably due to the residual stresses produced locally in the plate by the welding processes used in fabricating the specimen. Upon unloading, the experimental behavior seems to have a portion of vertical (infinitely stiff) response, which is probably just an artifice of the sensor and mounting technique used to in the measurement.

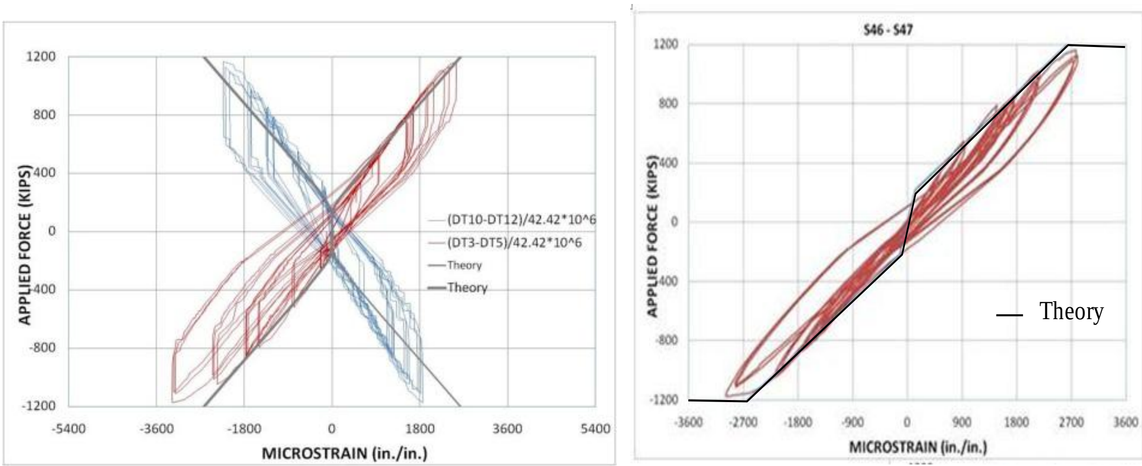

(a) Shear Force vs. Shear Strain in Flange (b) Shear Force vs. Shear Strain in Web

Figure 9. Comparison of Experimental and Theoretical In-Plane Shear Behavior

CONCLUSIONS

The in-plane shear behavior of SC composite walls can be represented using a tri-linear shear force-shear strain response based on a simple mechanics based model. The model explicitly accounts for the composite section behavior before cracking and the cracked orthotropic composite behavior after cracking. The cracking threshold corresponds to a concrete principal stress of $2(f'_c)^{0.5}$ in psi, which includes the effects of locked in shrinkage strains and discrete composite action. The in-plane shear strength corresponds to the limit state of Von Mises yielding of the steel plates.

Experimental results from tests conducted in Japan correlate well with the mechanics based tri-linear shear force-shear strain response. An additional large-scale cyclic in-plane shear test was conducted by the authors to further compare with the simple model. The test was conducted using a unique setup and specimen design. The experimental results compare reasonably with the model. There are some minor discrepancies due to the cyclic nature of the loading and the complexities of the loading and boundary conditions involved in conducting the tests.

Overall, the in-plane shear behavior of SC composite walls can be predicted reasonably and conservatively using the tri-linear shear force-shear strain response based on the simple mechanics based model.

ACKNOWLEDGMENTS

Testing at Purdue University was partially funded by Westinghouse Electric Company LLC. All opinions expressed in this paper are strictly those of the authors.

REFERENCES

[1] Ozaki, M., Akita, S., Oosuga, H., Nakayama, T., Adachi, N. (2004). "Study on Steel Plate Reinforced Concrete Panels Subjected to Cyclic In-Plane Shear." *Nuclear Engineering and Design*, Vol. 228, pp. 225-244.

[2] Varma, A.H., and Malushte, S., (2009). "In-Plane Behavior of Concrete Filled Steel (CFS) Elements." *Presentation. Enclosure 1 to DCP_NRC_00278*. Electronic ADAMS, NRC. Item ID 100130037. Accession Number ML 100050190. http://adamswebsearch2.nrc.gov/IDMWS/ViewDocByAccession.asp?AccessionNumber=ML100050190

[3] ACI 318-08, "Building Code Requirements for Structural Concrete and Commentary", American Concrete Institute, Farmington Hills, MI 2008.

[4] AISC 360-05, "Specification for Structural Steel Buildings", 13 Edition, American Institute of Steel Construction, Chicago, IL, 2005.